Whole Cell Target Engagement Identifies Novel Inhibitors of *Mycobacterium tuberculosis* Decaprenylphosphoryl-β-D-ribose Oxidase

Sarah M. Batt,[†] Monica Cacho Izquierdo,[‡] Julia Castro Pichel,[‡] Christopher J. Stubbs,[#] Laura Vela-Glez Del Peral,[§] Esther Pérez-Herrán,[‡] Neeraj Dhar,[Δ] Bernadette Mouzon,[#] Mike Rees,[#] Jonathan P. Hutchinson,[#] Robert J. Young,[⊥] John D. McKinney,[Δ] David Barros Aguirre,[‡] Lluis Ballell,*,[‡] Gurdyal S. Besra,*,[†] and Argyrides Argyrou*,[#]

[†]School of Biosciences, University of Birmingham, Birmingham B15 2TT, United Kingdom

[‡]Diseases of the Developing World and [§]Centro de Investigación Básica, Tres Cantos Medicines Development Campus, GlaxoSmithKline, Severo Ochoa 2, Tres Cantos, Madrid, Spain

[#]Department of Biological Sciences and [⊥]Department of Chemical Sciences, Molecular Discovery Research, Platform Technology and Science, GlaxoSmithKline, Stevenage SG1 2NY, United Kingdom

[Δ]School of Life Sciences, Swiss Federal Institute of Technology in Lausanne (EPFL), CH-1015 Lausanne, Switzerland

Ⓦ *Web-Enhanced Feature* Ⓢ *Supporting Information*
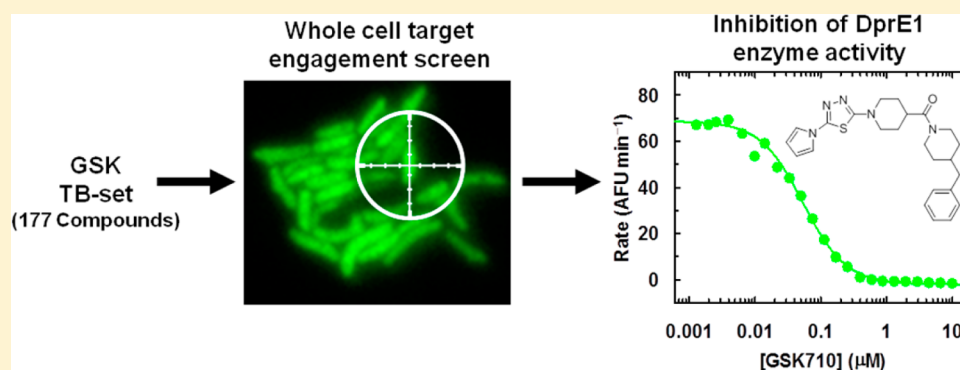
ABSTRACT: We have targeted the *Mycobacterium tuberculosis* decaprenylphosphoryl-β-D-ribose oxidase (Mt-DprE1) for potential chemotherapeutic intervention of tuberculosis. A multicopy suppression strategy that overexpressed Mt-DprE1 in *M. bovis* BCG was used to profile the publically available GlaxoSmithKline antimycobacterial compound set, and one compound (GSK710) was identified that showed an 8-fold higher minimum inhibitory concentration relative to the control strain. Analogues of GSK710 show a clear relationship between whole cell potency and in vitro activity using an enzymatic assay employing recombinant Mt-DprE1, with binding affinity measured by fluorescence quenching of the flavin cofactor of the enzyme. *M. bovis* BCG spontaneous resistant mutants to GSK710 and a closely related analogue were isolated and sequencing of ten such mutants revealed a single point mutation at two sites, E221Q or G248S within DprE1, providing further evidence that DprE1 is the main target of these compounds. Finally, time-lapse microscopy experiments showed that exposure of *M. tuberculosis* to a compound of this series arrests bacterial growth rapidly followed by a slower cytolysis phase.

KEYWORDS: *multicopy suppression, target overexpression, time-lapse microscopy, drug discovery*

D espite the existence of effective treatments for drug-sensitive tuberculosis (TB) and some important recent additions to the antibiotic arsenal against multidrug-resistant (MDR) forms of the disease,[1] TB still accounts for nearly 9 million new infections and over 1 million deaths each year.[2] Combined with the increasing prevalence of MDR-TB[3] and the often fatal comorbidity between TB and human immunodeficiency virus (HIV), the discovery of new chemical entities with novel modes of action is a high priority in the global health agenda. Ideally, a new drug should shorten the duration of

treatment, have a clean safety profile, avoid significant drug–drug interactions with new or established regimens (TB and HIV), treat both MDR and extremely drug-resistant TB (XDR-TB), and be competitive in terms of cost with current standards of care.
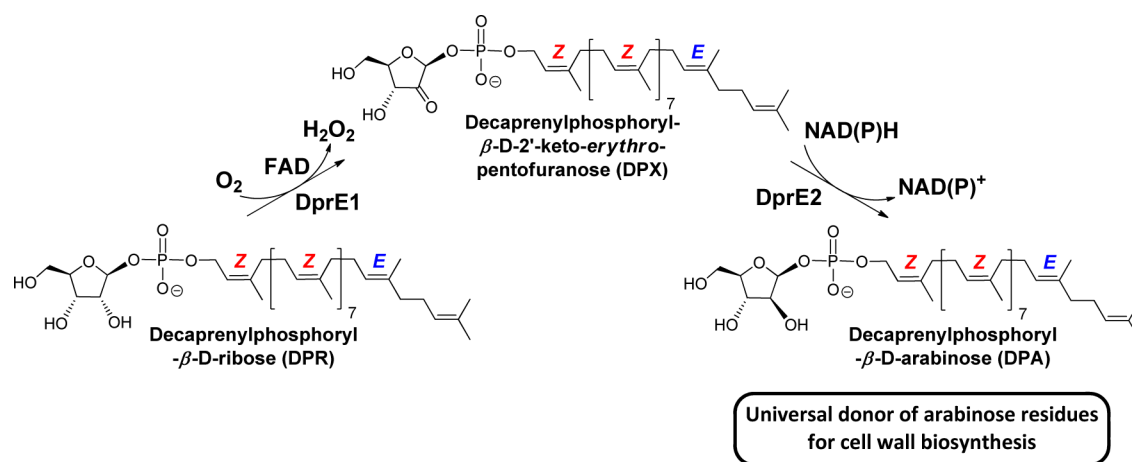
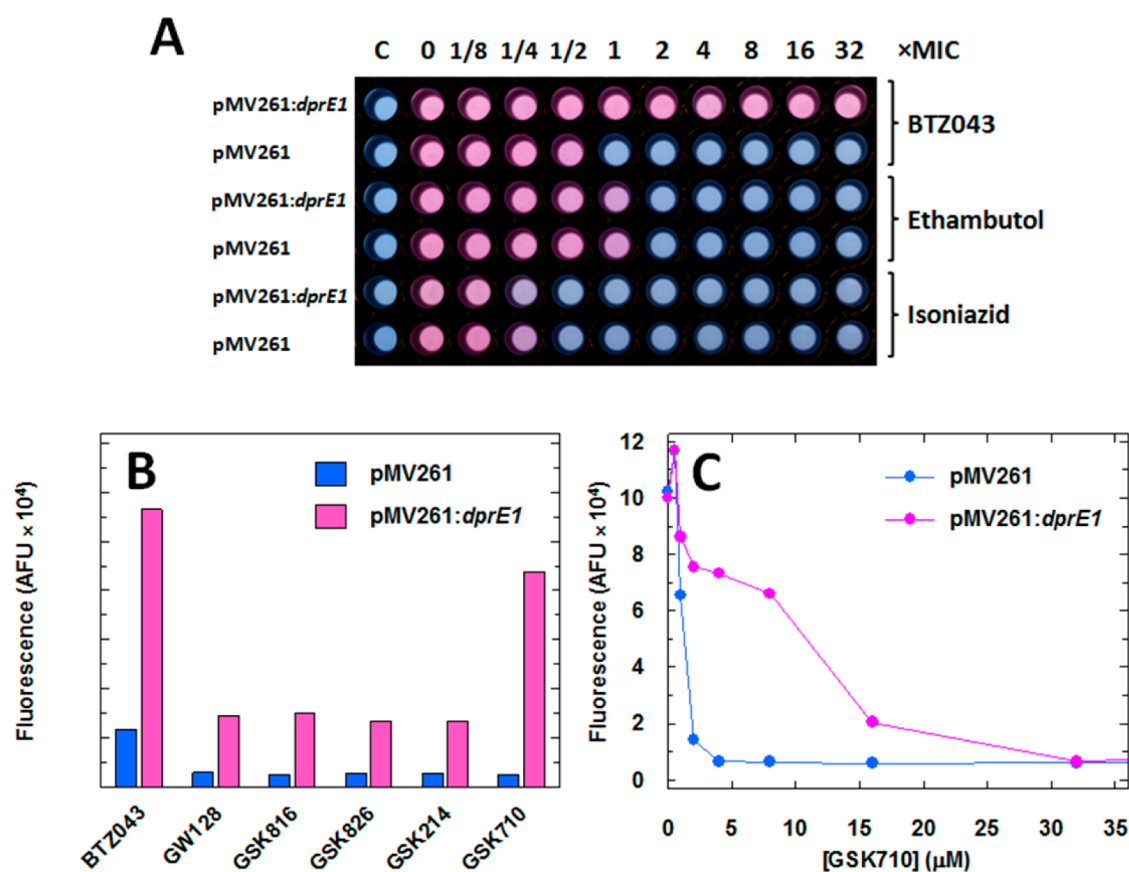**Figure 1.** Reactions catalyzed by DprE1 and DprE2.

Figure 2. Multicopy suppression screen of the TB-set. (A) Assay is validated by demonstrating that overexpression of Mt-DprE1 in *M. bovis* BCG confers a >32-fold increase in resistance to BTZ043 but no resistance to ethambutol or isoniazid. *M. bovis* BCG transformed with pMV261 (empty vector) or pMV261:*dprE1* were grown in Middlebrook 7H9 media supplemented with 10% (v/v) OADC, 25 μg/mL kanamycin, and the indicated compound concentrations expressed as fold-× of the MIC of each compound. Pink indicates viable cells, and blue indicates nonviable cells. (B) Multicopy suppression screen of the TB-set at 2× MIC of each compound identifies GSK710 as a putative inhibitor of Mt-DprE1. Overexpression of Mt-DprE1 in *M. bovis* BCG permits cells to grow significantly better in the presence of GSK710 and the positive control (BTZ043) but mildly better in the presence of the other four compounds. (C) Overexpression of Mt-DprE1 in *M. bovis* BCG confers an 8-fold increase in resistance to GSK710.

Essential to the goal of targeting MDR and XDR-TB is the identification and exploitation of new molecules unencumbered by pre-established clinical resistance mechanisms. We and others have explored a number of different strategies that include whole cell assays[4−6] and rational target-based screening.[7] The public release of hit compounds identified after systematic anti-mycobacterial screens against compound repositories generates new public−private collaborative opportunities for mode of action studies and subsequent target-based discovery programs.[8]

Mycobacterium tuberculosis decaprenylphosphoryl-β-D-ribose oxidase (Mt-DprE1, Figure 1) catalyzes the flavin adenine dinucleotide (FAD) dependent oxidation of decaprenylphosphoryl-β-D-ribose (DPR) to decaprenylphosphoryl-β-D-2′-keto-*erythro*-pentafuranose (DPX). DPX is subsequently reduced to

Table 1. Correlation between Inhibition of DprE1 Enzyme Activity, Binding Affinity, and Cellular Potency by GSK710 and Analogues

Compound	Structure	IC$_{50}$ (µM)[a]	K_d (µM)[b]	MIC (µM)[c]	OE MIC (µM)[d]	MIC Foldshift[e]	CLND Solubility (µM)	Chrom logD pH 7.4
GSK710		0.054 ± 0.002	0.25 ± 0.09	4	>125	>32	≤1	6.37
GSK058		0.054 ± 0.003	0.16 ± 0.10	4	>125	>32	14	6.41
GSK305		0.26 ± 0.01	ND[f] (Interference)	31	>125	>4	21.5	5.36
GSK310		0.40 ± 0.03	1.1 ± 0.4	4	125	32	64	4.99
GSK059		0.44 ± 0.04	1.0 ± 0.4	4	125	32	416	4.01
GSK763		1.2 ± 0.1	ND (Interference)	16	>125	>8	208	5.24
GSK303		1.7 ± 0.1	1.6 ± 0.3	16	>125	>8	328	5.09
GSK155		2.6 ± 0.2	2.3 ± 0.6	63	>125	>2	276	4.12
GSK717		3.6 ± 0.2	2.4 ± 0.3	63	>125	>2	250	4.61
GSK018		21 ± 2	6.8 ± 2.0	>125	ND	NA[g]	445	2.83
GSK074		>100	Fluorescence change not observed	>125	ND	NA	318	1.42
GSK944		>100	Fluorescence change not observed	>125	>125	NA	322	1.33

[a]The IC$_{50}$ values are from the fits of the data in Figure 3D. [b]Apparent K_d values from the fits of the FAD fluorescence quenching data in Figure 4B. [c]MIC values are for *M. tuberculosis* transformed with pMV261. [d]Overexpressor (OE) MICs are for *M. tuberculosis* transformed with pMV261:*dprE1*. [e]Ratio of MIC values for *M. tuberculosis* transformed with pMV261:*dprE1* to that for *M. tuberculosis* transformed with pMV261. [f]Not determined. [g]Not applicable.
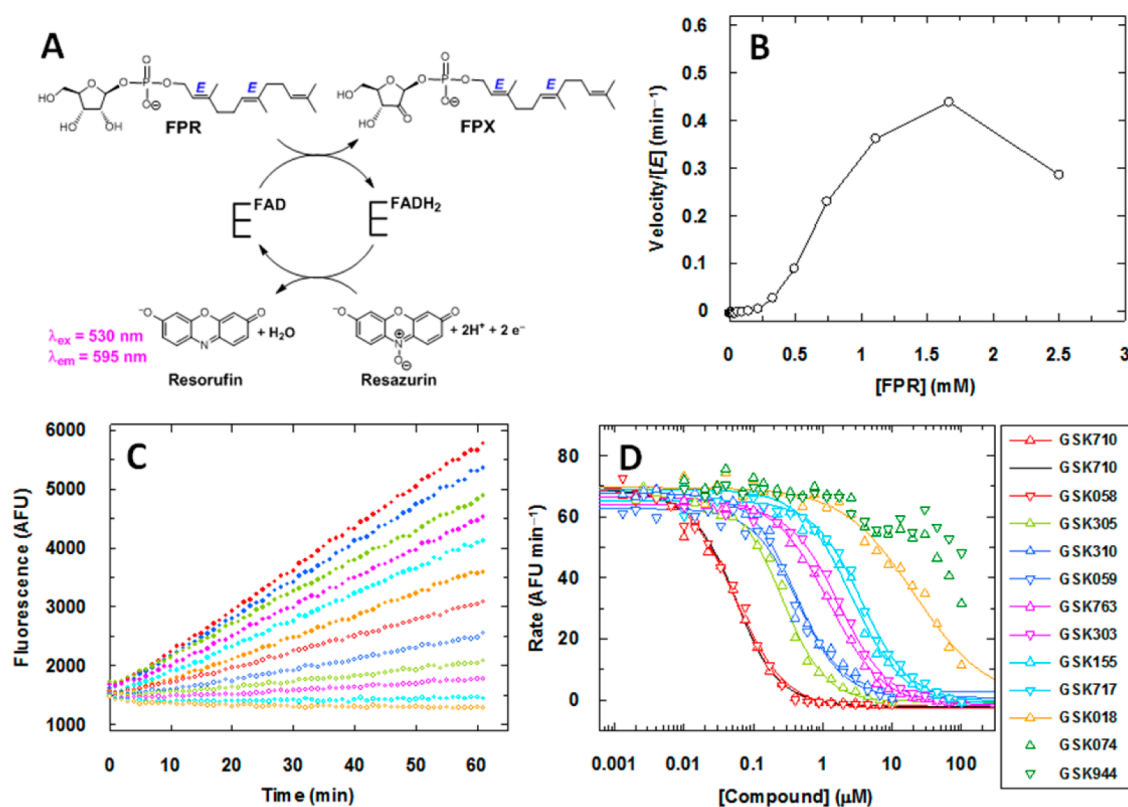
Figure 3. Enzyme assay development and inhibition of Mt-DprE1 by GSK710 and analogues. (A) Redox cycling enzymatic assay principle for Mt-DprE1. As FPR is oxidized to FPX, resazurin is reduced to resorufin and can be monitored by an increase in fluorescence intensity at 595 nm. E-FAD and E-FADH$_2$ denote oxidized enzyme and two-electron reduced enzyme, respectively. (B) Rate–FPR concentration relationship. Assays contained 500 nM Mt-DprE1, 50 μM resazurin, and increasing FPR concentration. Velocity/[E] (min^{-1}) represents moles of resorufin product formed per mole of enzyme per minute. (C) Time courses illustrating reaction linearity for up to 60 min and inhibition of enzyme activity by GSK710. 1300 AFU corresponds to 1 μM resorufin. Assays contained 250 nM Mt-DprE1, 1 mM FPR, 50 μM resazurin, and increasing concentrations of GSK710. (D) Dose–response curves for GSK710 and 11 analogues. The solid lines are fits to eq 1, and the black line is the fit of the GSK710 data to eq 2. Assays contained 250 nM Mt-DprE1, 1 mM FPR, 50 μM resazurin, and increasing concentrations of the indicated compounds.

decaprenylphosphoryl-β-D-arabinose (DPA) by the reduced pyridine nucleotide dependent enzyme, DprE2.[9] DPA is the sole donor of arabinose residues for the essential cell wall components, arabinogalactan and lipoarabinomanan.[9-11] Mt-DprE1 has been genetically validated as a drug target using gene knockout and knock-down technologies,[12] and its extracytoplasmic localization makes it particularly vulnerable to inhibition by small molecules.[13] Mt-DprE1 has been shown to be the target of the mechanism-based suicide inhibitor class of nitroaromatic compounds, of which BTZ043 has been demonstrated to be an effective anti-TB compound in mice.[14,15] Several cell-active reversible inhibitors of Mt-DprE1 have also been identified recently,[16-22] suggesting that Mt-DprE1 is a highly tractable target for chemotherapeutic intervention.

To bring together target-based and phenotypic screening strategies, we considered the use of genetic tools that could help systematically assign compounds with attractive anti-TB properties to specific targets of interest. This would minimize some of the limitations associated with progressing hits to leads and lead optimization programs based solely on minimum inhibitory concentration (MIC) determinations. These include the lack of guidance from structural biology and in vitro compound profiling and mechanism of action studies, the difficulties associated with identifying toxicological liabilities, and the somewhat unpredictable nature of mycobacterial small molecule permeability, resulting in confounded structure–activity relationship analyses and pursuit of molecules with poor physicochemical proper-

ties.[23] The screening of a privileged set of published compounds with attractive anti-TB activity against an Mt-DprE1 overexpressor strain should make possible the assignment of compound–target pairs of interest by means of a MIC shift observed when wild type and overexpressor strains are compared. This multicopy suppression method was successfully applied first in *Escherichia coli*[24] followed shortly thereafter in *Saccharomyces cerevisiae*.[25] The identification of novel Mt-DprE1 inhibitors would allow medicinal chemists access to biochemical and structural biology support to guide future lead optimization efforts in addition to helping to identify potential toxicological risks associated with a particular target class.

In this paper, we describe how the combined use of phenotypic and target-based approaches for Mt-DprE1 has led to the identification of a new lead series for TB.

RESULTS

Multicopy Suppression Screen of the TB-Set. Phenotypic screening of the GlaxoSmithKline (GSK) compound library has previously identified a collection of 177 compounds that inhibited the growth of *M. tuberculosis* with MIC values of <10 μM and a therapeutic index (HepG2 IC$_{50}$/MIC) of > 50, which we have termed the "TB-set".[4] Because the phenotype of the screen was cell viability, the targets of the TB-set are largely unknown. To identify inhibitors of Mt-DprE1 that might be present in the TB-set, we employed two screening strategies: a
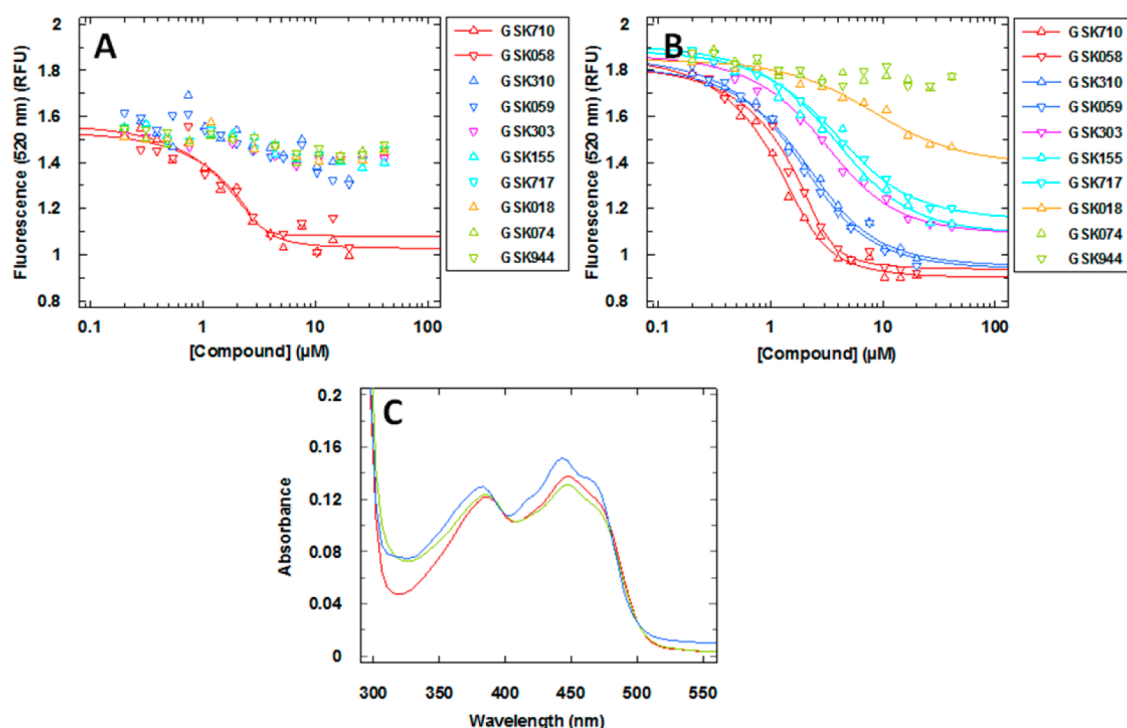
Figure 4. Mechanism of binding of GSK710 and analogues to Mt-DprE1. FAD cofactor fluorescence quenching by GSK710 and analogues in the absence (A) and presence of 500 μM FPR (B). Assays contained 2.9 μM Mt-DprE1 and increasing concentrations of the indicated compounds. The solid lines are fits to eq 3. (C) UV−visible absorbance spectra for 10 μM Mt-DprE1 (red), 10 μM Mt-DprE1 and 500 μM FPR (5 min incubation, green), and 10 μM DprE1, 500 μM FPR, and 20 μM GSK059 (5 min incubation, blue). The contribution of 20 μM GSK059 to the absorbance spectrum of the latter was subtracted.

multicopy suppression approach and a traditional enzymatic assay approach that monitors catalytic turnover.

Mt-*dprE1* was cloned into the plasmid pMV261[26] to generate pMV261:*dprE1* and introduced into *Mycobacterium bovis* BCG. This host−plasmid system permits constitutive expression of target proteins. After the bacteria have been incubated in the presence of compound for 7 days, cell viability can be assessed by the ability of endogenous reductases to reduce resazurin to resorufin.[27] As a proof of concept, cells transformed with pMV261:*dprE1* grew in the presence of BTZ043 with an MIC >32-fold higher than that when cells were transformed with empty vector (Figure 2A). Cells transformed with pMV261:*dprE1* did not confer any growth advantage over cells transformed with vector alone when cells were grown in the presence of ethambutol or isoniazid, two anti-mycobacterial-specific compounds that do not inhibit Mt-DprE1.[2]

Having validated that this assay can identify inhibitors that are specific to Mt-DprE1, we proceeded to screen the TB-set at twice the previously measured MIC value of each compound. Figure 2B shows that overexpression of Mt-DprE1 in *M. bovis* BCG conferred resistance to five compounds of the TB-set compared to the empty vector. The MIC values for these five compounds were then measured to determine if there was a shift in the MIC when Mt-DprE1 was overexpressed. Of these five compounds, GSK710 showed an 8-fold shift in the MIC when Mt-DprE1 was overexpressed in *M. bovis* BCG (Figure 2C), whereas the remaining four compounds showed a ≤2-fold shift in the MIC and this was considered not to be significant. The MIC values for GSK710 and 11 structural analogues were measured in *M. tuberculosis* carrying pMV261 or pMV261:*dprE1*, and these are shown in Table 1.

Enzyme Assay for Mt-DprE1. We developed a redox cycling enzyme assay for Mt-DprE1 that uses farnesylphosphor-yl-β-D-ribose (FPR) and resazurin as substrates and generates farnesylphosphoryl-β-D-2′-keto-*erythro*-pentafuranose (FPX) and resorufin as products (Figure 3A). Figure 3B shows that Mt-DprE1 catalyzes the FPR-dependent reduction of resazurin to resorufin, although the rate−FPR concentration relationship is complex; there is a sigmoidal dependence at low FPR concentration reaching a maximal apparent turnover number of approximately 0.45 min^{-1} and apparent substrate inhibition at high FPR concentration. A sigmoidal dependence of the rate on FPR concentration has also been reported for the *M. smegmatis* DprE1.[28] Analytical ultracentrifugation studies suggest that Mt-DprE1 is a monomer in solution and, therefore, cooperative binding of substrate to the enzyme is difficult to rationalize in the context of a monomeric enzyme with a single active site.[15] The reasons for this complex rate−FPR concentration relationship are, therefore, not clear at the present time. Figure 3C shows progress curves performed in the presence of 1 mM FPR and 250 nM Mt-DprE1 and increasing concentration of GSK710. The resorufin product forms linearly with time up to 60 min, and the rate of the reaction is inhibited by GSK710, yielding an IC$_{50}$ value of 54 nM (Figure 3D and Table 1). Also shown in Figure 3D is the dose−response curves for the 11 analogues, and the IC$_{50}$ values are also given in Table 1.

Effect of Compounds on the Optical Properties of the FAD Cofactor. The mechanism of compound binding to Mt-DprE1 was probed by monitoring changes in the FAD cofactor environment by fluorescence. In the absence of FPR, the two most potent compounds (GSK710 and GSK058) show significant quenching of FAD fluorescence, whereas the other compounds do not (Figure 4A). In the presence of 500 μM FPR,

Table 2. Minimum Inhibitory Concentrations (MIC) of *M. bovis* BCG Spontaneous Mutants[a]

Compound	Structure	WT	*recG*[b]	WT[b] DprE1 E221Q	*recG*[b] DprE1 E221Q	*recG*[b] Dpre1 G248S
GSK710		1.6	1.6	25	25	6.25
GSK303		50	50	400	400	200
TCA1		3.1	3.1	25	25	12.5
BTZ043		0.009	0.009	0.018	0.018	0.004

[a]MICs (μM) were determined from the graphs in Figure S1. [b]*recG* DprE1 E221Q and *recG* DprE1 G248S refer to spontaneous mutants in DprE1 generated using the *M. bovis* BCG *recG* mutant strain, and WT DprE1 E221Q refers to spontaneous mutants generated using the wild type *M. bovis* BCG strain.
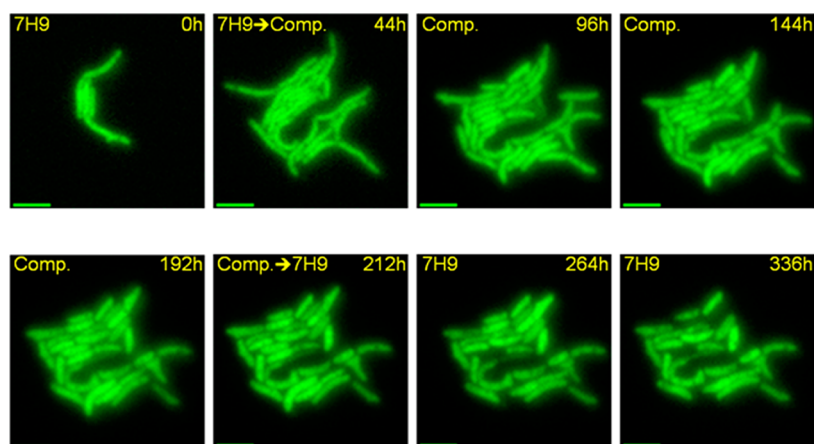
Figure 5. Single-cell analysis of the effect of GSK059 on *M. tuberculosis*. Representative image series of *M. tuberculosis* expressing GFP, grown in a microfluidic device and exposed to 40 μM GSK059 between 44 and 212 h, after which the drug was washed out. The flow medium is indicated on the top left of the images (7H9 denotes complete 7H9 medium; Comp. denotes complete 7H9 medium containing 40 μM GSK059). Numbers on the top right of the images indicate the hours elapsed. The scale bar shown represents 3 μm.

all compounds show quenching of FAD fluorescence except for the two weakest compounds, GSK074 and GSK944 (Figure 4B). Figure 4C shows the absorbance spectrum of the FAD cofactor bound to Mt-DprE1 in the absence and presence of turnover and of enzyme inhibited by GSK059. The latter compound was selected for this experiment rather than the original hit because of its reasonable potency and improved aqueous solubility (Table 1).

Enzymatic Assay Screen of the TB-Set. The TB-set was also screened using the enzymatic assay at a single compound concentration of 10 μM. From the 177 compounds, 29 showed >30% inhibition and were selected for 11-point dose−response analysis using 100 μM as the top concentration. Of the 29 compounds tested, 20 showed dose−response curves that could be fitted to eq 1, yielding IC$_{50}$ values of <100 μM. The distribution was as follows: 11 compounds showed IC$_{50}$ values between 10 and 60 μM, 7 compounds between 3 and 10 μM, and 2 compounds <1 μM. One of the compounds with IC$_{50}$ < 1 μM

was GSK710. Compounds with IC$_{50}$ values <10 μM are shown in Table S1.

Generation of *M. bovis* BCG Spontaneous Mutants Resistant to GSK710 and GSK303. *M. bovis* BCG and *M. bovis* BCG *recG* strains were plated at 2.5, 5, and 10 times the MIC values for GSK710 and the analogue, GSK303. At 5 times the MIC, spontaneous resistant mutants to GSK710 and GSK303 were isolated at a frequency of 10 and 13 per 10^8 cells, respectively, for the *M. bovis* BCG strain. For the *M. bovis* BCG *recG* mutant strain, spontaneous resistant mutants appeared at a frequency of 6 per 10^8 cells at 5 times the MIC of GSK710 and 170 per 10^8 cells at 2.5 times the MIC of GSK303. Sequencing of the *dprE1* open reading frame of 10 resistant mutants revealed that each mutant had one of two single nucleotide mutations. The first had a G → C mutation at nucleotide 661 (^{661}GAA^{663} → ^{661}CAA^{663}) and the second had a G → A mutation at nucleotide 742 (^{742}GGC^{744} → ^{742}AGC^{744}), resulting in E221Q or G248S mutations, respectively. The MICs of the mutants were compared to those of the parental strains for GSK710 and

GSK303 and for the structurally unrelated inhibitors, TCA1[21] and BTZ043[14] (Table 2 and Figure S1). Both mutations conferred resistance to GSK710 (16-fold for E221Q and 4-fold for G248S), GSK303 (8-fold for E221Q and 4-fold for G248S), and TCA1 (8-fold for E221Q and 4-fold for G248S), but no or minimal resistance to BTZ043 (2-fold for E221Q and 0.5-fold for G248S).

Time-Lapse Microscopy. To evaluate the bactericidal activity of the GSK710 compound series, we carried out time-lapse microscopy on *M. tuberculosis* grown in a microfluidic device.[29] Bacteria were initially grown until they formed small microcolonies, after which they were exposed to 40 μM GSK059 (10 times the MIC) for 7 days. Upon addition of compound, the cells decreased their growth rate quite dramatically, even though cell divisions continued for some time (Figure 5; Movie S1). However, cell lysis was delayed, starting only after about 4 days of drug exposure as evidenced from an abrupt loss of GFP signal, and continued after washout of the compound between 212 and 340 h (Figure 5; Movie S1). The delay in cytolysis is similar to that observed with the 4-aminoquinoline piperidine amide (AQ) inhibitor of DprE1 described recently[17] but different from the killing induced by BTZ043,[14] where the lysis was much more rapid and pronounced. Also, unlike BTZ043 and AQ, exposure of *M. tuberculosis* to GSK059 did not result in pleomorphic changes in bacterial shapes, even though some cells appeared to release their cytoplasmic contents from regions near the poles (Movie S1, phase channel).

■ DISCUSSION

Target overexpression is a clinically observed mechanism of bacterial resistance to antibiotics.[30−32] Resistance in these cases arises because inhibition of essential cellular processes is overcome by overexpression of the target. Target overexpression can occur through point mutations in gene promoters resulting in increased transcription and translation. For example, mutation in the promoter of the *M. tuberculosis inhA* gene is a mechanism of clinical resistance to isoniazid, a key drug used to treat TB.[30] In the laboratory, overexpression of proteins can be accomplished using plasmids that overexpress these genes, and this strategy has been successfully applied to demonstrate antibiotic resistance by way of shifts in MIC values.[14,33,34] Shifts in MIC values caused by target overexpression, therefore, can provide a simple measure of target engagement at the cellular level, which is extremely valuable information for drug discovery programs from the early hit identification stage and well into lead optimization.[35,36]

Prior successes utilizing target overexpression in hit identification campaigns in *Escherichia coli*[24] and *Saccharomyces cerevisiae*,[25] encouraged us to use this approach to profile GSK's TB-set of compounds for whole cell active inhibitors of Mt-DprE1 and identified one compound, GSK710, that showed an 8-fold shift in the MIC when Mt-DprE1 was overexpressed in *M. bovis* BCG. MIC shifts alone, however, are insufficient evidence for target engagement. MIC shifts can also arise through nontarget mechanisms such as covalent modification of the compound by the overexpressed protein that renders it inactive.[37] Evidence of inhibition of Mt-DprE1 enzyme activity was additionally required to establish a link between MIC shift and cellular target engagement. We, therefore, developed an enzymatic assay using FPR as substrate, which differs significantly from the physiological substrate in terms of both length and geometric isomer configuration of double bonds in the polyisoprenoid chain (see Figures 1 and 3A).[10] Despite these differences, the *Mycobacterium smegmatis* DprE1 has previously

been shown to catalyze turnover of FPR,[28] which encouraged us to explore an FPR-based enzymatic assay for Mt-DprE1 given that the physiological substrate is not available or readily synthesized.

Two assays have previously been developed for *M. smegmatis* DprE1.[28] The first assay monitors the oxidase activity of DprE1 by coupling the hydrogen peroxide product (Figure 1) to horseradish peroxidase and amplex red, resulting in the formation of resorufin, which can be monitored by a change in absorbance or fluorescence. The second assay takes advantage of the diaphorase activity that many flavin-dependent enzymes possess and monitors reduction of dicholorophenolindophenol by absorbance. Although both assays were suitable, an alternative direct assay that avoids the use of coupling enzymes and possesses the required sensitivity to enable miniaturization was desired. We tested resazurin as an alternative electron acceptor, which upon reduction regenerates resorufin. GSK710 inhibits Mt-DprE1 with an IC_{50} of 54 nM (Figure 3D), suggesting that Mt-DprE1 is the primary target of this compound. The measured IC_{50} value is 5-fold lower than the enzyme concentration used in the assay, suggesting that this value may not be accurate due to tight-binding limit considerations. The same data were, therefore, fitted to eq 2 to allow for compound depletion that could arise due to the tight-binding conditions of the assay, yielding an apparent K_i of 25 nM (Figure 3D, black line).[38] This analysis additionally calculates an active enzyme concentration of 60 nM, suggesting that the enzyme is approximately 25% fractionally active under the assay conditions. The low maximal turnover number of 0.45 min^{-1} for Mt-DprE1 using the FPR substrate, therefore, probably reflects the nonphysiological nature of this substrate rather than largely inactive recombinant enzyme.

Having confirmed that Mt-DprE1 is inhibited by GSK710, analogues were tested to improve the suboptimal physicochemical properties of the original hit (high Chrom Log$D_{7.4}$ and no measurable solubility). As shown in Table 1, changes can be tolerated on the terminal phenyl group including addition of fluorine at the para position and replacement with pyridine regioisomers and other functional groups, as well as removal, resulting in dramatic increases in solubility and improved distribution coefficients while maintaining inhibitory activity. The modifications result in a wide range of enzymatic IC_{50} values that correlate with *M. tuberculosis* MIC values, and the analogues stay on target as evidenced by the observed MIC shifts between the wild type and the Mt-DprE1 overexpressor strain. It should be noted that the compound series represented by GSK710 is structurally distinct from previously identified DprE1 inhibitors TCA1,[21] BTZ043,[14] AQ,[17] pyrazolopyridones,[18] and 1,4-azaindole.[16,19]

Screening of the TB-set using the enzymatic assay identified a number of other compounds with measured IC_{50} values in the 0.8−10 μM range, which were not identified using the multicopy suppression approach (Table S1). However, more lead validation work would be required before these compounds might qualify as bona fide inhibitors of Mt-DprE1 for one or more of the following reasons: (1) poor compound solubility relative to the enzymatic IC_{50} values (GSK678 and GSK671); (2) minimal or no loss in potency going from the enzymatic assay to the cell viability assay (GSK389 and GSK9310), suggesting that these compounds may have additional targets; and (3) minimal or no shift in the MIC between the wild type and the Mt-DprE1 overexpressor (GSK703, GSK960, and GSK553), also suggesting that these compounds may have additional targets. GSK703, GSK553, and GSK684 have a common pyridinyl thiazole amine

moiety, suggesting that a DprE1-specific compound series could emerge through further chemistry.

The complex rate–FPR relationship shown in Figure 3B precludes determining the mechanism of inhibition of Mt-DprE1 by inhibitors using full pattern inhibition analysis. We therefore examined changes in the optical properties of the FAD cofactor as an alternative means of obtaining information about the mechanism of compound binding to Mt-DprE1. The fluorescence of the FAD cofactor bound to Mt-DprE1 is quenched approximately 20-fold relative to FAD in solution. Displacement of the FAD by compound as a potential mechanism of inhibition can be ruled out because an increase in FAD fluorescence upon addition of compound is not observed, regardless of whether FPR is present or not (Figure 4A,B). Except for the two most potent compounds, FPR seems to be required to observe FAD fluorescence quenching. Given that Mt-DprE1 is undergoing turnover in the presence of FPR via the oxidase activity during these measurements, in principle, compounds could inhibit Mt-DprE1 by binding to any of the intermediates during the catalytic cycle, including the resting state of the enzyme (E-FAD), the Michaelis complex (E-FAD:FPR), or the reduced flavin intermediate either before (E-FADH$_2$:FPX) or after (E-FADH$_2$) dissociation of the FPX product. A significantly reduced absorbance in the 450 nm range is expected if compounds inhibit Mt-DprE1 by trapping the enzyme in the two-electron reduced form. Instead, in the presence of FPR and GSK059, the FAD remains oxidized and the spectrum is characterized by a blue shift in the maximal absorbance from 448 to 444 nm and the emergence of a shoulder at 470 nm, which suggests binding of the isoalloxazine ring of the FAD in a more hydrophobic environment (Figure 4C).[39] Therefore, this class of compounds inhibits Mt-DprE1 by binding to E-FAD or the Michaelis complex, and our data, at present, cannot distinguish between these two possibilities. Finally, there is a good correlation between inhibition of enzymatic activity (IC$_{50}$) and apparent binding affinity (K$_d$) measured by FAD fluorescence quenching in the presence of FPR (Table 1).

Isolation of spontaneous resistant mutants to antibiotics has proven to be a successful method of target identification including the identification of Mt-DprE1 as the target of BTZ043.[14] We used this strategy as an independent and completely unbiased method of identifying the target(s) of GSK710 and isolated *M. bovis BCG* spontaneous resistant mutants to GSK710 and GSK303. All 10 of the randomly selected mutants had a single point mutation at two sites, E221Q or G248S within DprE1, suggesting that DprE1 is the main target of these compounds. These mutants also show cross-resistance to TCA1 but minimal or no resistance to BTZ043, two active-site inhibitors of DprE1 (Table 2). The residues E221 and G248 are located in the substrate-binding domain of the protein but far from the active-site pocket (Figure 6). Despite repeated attempts, we have not succeeded in obtaining a crystal structure of Mt-DprE1 with a compound from the GSK710 series bound, which makes interpretation of how mutation of these residues could affect compound binding difficult.

In conclusion, we have harnessed the combined power of phenotypic and target-based approaches and identified a new lead series that inhibits Mt-DprE1 with nanomolar affinity, arrests bacterial growth at low micromolar concentration, and is bactericidal. Exemplars are in good chemical space and amenable to further chemistry, with the potential of a new drug emerging to combat both drug-sensitive and multidrug-resistant tuberculosis.
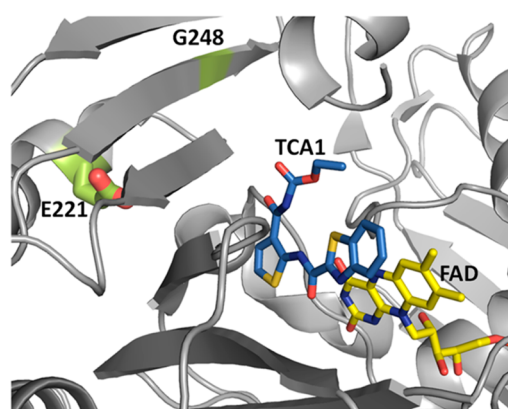
Figure 6. Mt-DprE1 structure with TCA1 bound (PDB ID 4KW5) illustrating the position of residues E221 and G248 relative to the active site pocket.

■ METHODS

Materials. All chemicals and buffers were of analytical or reagent grade and were used without further purification unless otherwise stated. Flavin adenine dinucleotide (FAD) was from Sigma, resazurin and resorufin were from Life Technologies, *Bam*HI and *Hin*dIII restriction enzymes and Tween-20 were from Thermo Scientific, and Quick-stick ligase was from Bioline. Isoniazid and ethambutol were from Sigma-Aldrich, BTZ043 was from Selleckchem, and TCA1 was from Life Chemicals.

General Chemical Syntheses Methods. Reactions were monitored by thin layer chromatography (TLC) using Merck 60 F254 silica gel glass backed plates, and elution was visualized by UV light. Reactions were also monitored by liquid chromatography–mass spectrometry (LC-MS) using an Agilent 1100 LC system equipped with a photo diode array detector and a Waters ZMD 2000 high-resolution mass spectrometer. Compounds were purified by column chromatography or preparative high-performance liquid chromatography (HPLC). Automated flash chromatography was performed on a Flash Biotage Isolera SP4 system, and preparative HPLC was performed on an Agilent 1100 or 1200 with peak detection. All NMR spectra were recorded on a Bruker DPX Avance 400 MHz instrument equipped with a quattro nucleus probe. Measurements were made at room temperature in an appropriate deuterated solvent using the residual solvent hydrogen resonances as standards (d_6-DMSO, δ = 2.50 ppm; CDCl$_3$, δ = 7.27 ppm; CD$_3$OD, δ = 3.31 ppm). Chemical shifts are expressed in parts per million (ppm, δ units). Coupling constants (J) are in units of hertz (Hz). Splitting patterns describe apparent multiplicities and are designated s (singlet), d (doublet), t (triplet), q (quartet), dd (double doublet), m (multiplet), and br (broad). Analytical purity was ≥95% unless stated otherwise and was determined by ^{1}H NMR and HPLC analyses. The purity of the final compounds was checked using a Waters 2795 HPLC system equipped with a Waters 2996 photo diode array detector and a Waters ZQ2000 mass spectrometer. All mass spectra were performed by electrospray ionization (ESI). Representative procedures and physical properties and characterization of the main compounds are described. The commercial sources and synthetic strategies of FPR and all compounds used in this study are described in the Supporting Information.

Cloning, Expression, and Purification. Cloning of Mt-DprE1 into plasmids pCDF-Duet and pMV261 and expression

and purification of Mt-DprE1 are detailed in the Supporting Information.

Enzyme Assay for DprE1. Oxidation of farnesylphosphoryl-β-D-ribose (FPR) to farnesylphosphoryl-β-D-2′-keto-*erythro*-pentafuranose (FPX) by DprE1 results in the formation of a two-electron reduced flavin intermediate ($FADH_2$). To complete the catalytic cycle, the $FADH_2$ has to be reoxidized to FAD. In the present assay, this can be accomplished by resazurin, which upon reduction generates the highly fluorescent product resorufin (Figure 3). Reactions were monitored by following an increase in fluorescence intensity (λ_{ex} = 530 nm, λ_{em} = 595 nm) associated with the formation of resorufin. Assays were carried out in black 384-well low-volume microplates (Greiner Bio-one, Stonehouse, UK; catalog no. 78076) and contained 50 mM Hepes, pH 7.5, 100 mM NaCl, 1.5% (v/v) DMSO, 100 μM Tween-20, 2 μM FAD, and 50 μM resazurin, with variable concentrations of FPR and DprE1 in a total reaction volume of 10 μL. Measurements were made using a Tecan Safire[2] instrument (Tecan Group Ltd., Seestrasse, Switzerland). Enzymatic rates in arbitrary fluorescence units per unit time were converted to quantity of product formed per unit time using a resorufin standard curve. For the 24-point dose−response curves of Figure 3D, DMSO solutions of compounds were dispensed using a Hewlett-Packard HP D300 digital dispenser (Tecan Group Ltd.).

FAD Cofactor Fluorescence Quenching by Compounds. Assays were performed in the same plate type as the enzymatic assay in a final volume of 10 μL. DMSO solutions of compounds were also dispensed using the Hewlett-Packard HP D300 digital dispenser giving a final DMSO concentration of 1% (v/v). Upon addition of 2.9 μM Mt-DprE1 in 50 mM Hepes, pH 7.5, 100 mM NaCl, and 100 μM Tween-20 to the compounds, the plates were sealed and incubated at room temperature, in the dark, for 1 h. Fluorescence intensity measurements were performed using a Tecan Safire[2] plate reader in fluorescence polarization mode (λ_{ex} = 470 nm, λ_{em} = 520 nm). Total fluorescence intensity was calculated from the parallel and perpendicular components and normalized relative to the intensity of a 125 nM FAD control.

Absorbance Spectra. UV−visible absorbance spectra were recorded on an Agilent 8453 UV−visible spectrophotometer (1 nm intervals; 0.5 s integration times) using a 1 mL Hellma QS282 quartz cuvette. A solution of 10 μM Mt-DprE1 and 500 μM FPR was pre-incubated for 5 min before its UV−visible spectrum was measured. To this solution was added 20 μM GSK059 (from a 2 mM stock solution in DMSO), and the UV−visible spectrum of this solution was measured after 5 min. All measurements were performed in 50 mM Hepes, pH 7.5, 100 mM NaCl, 100 μM Tween-20, and 1.5% (v/v) glycerol at 25 °C.

Enzymatic Assay Screen. Five microliters of a 2× substrate solution containing 1.2 mM FPR and 100 μM resazurin in assay buffer (50 mM Hepes, pH 7.5, 100 mM NaCl, 100 μM Tween-20, 2 μM FAD) was dispensed into the 384-well screening plates containing 100 nL of compound. Reactions were initiated by the addition of 5 μL of a 2× enzyme solution containing 1.2 μM Mt-DprE1, also in assay buffer. Plates were centrifuged at 1000 rpm for 1 min and the reactions incubated at room temperature for 2 h, before the fluorescence (λ_{ex} = 544 nm, 15 nm bandwidth filter; λ_{em} = 590 nm, 20 nm bandwidth filter) was measured on an Envision multilabel reader (PerkinElmer). All solutions were dispensed using a Multidrop Combi dispenser (Thermo Fisher Scientific, Waltham, MA, USA).

Multicopy Suppression Screen. Intermediate plates containing 1 and 0.1 mM compounds in DMSO were prepared in 96-well, flat-bottom, polystyrene plates. Two microliters of these compound solutions was transferred in duplicate to Greiner black-bottom assay plates. As a positive control, BTZ043 was added to one well to a final concentration of 4 ng/ μL. *M. bovis* BCG/pMV261 and pMV261:*dprE1* cells were grown at 37 °C in Middlebrook 7H9 medium supplemented with 10% (v/v) oleic albumin dextrose catalase (OADC, Sigma) and 25 μg/mL kanamycin. Exponentially growing cells were diluted to 1.5×10^6 colony-forming units (CFU)/mL in the same medium, and 98 μL of the diluted cells was added to the assay plates; the plates were sealed with parafilm and silver foil and incubated at 37 °C in a humid, CO_2 incubator. After a 7 day incubation period, 30 μL of 0.02% (w/v) resazurin and 12.5 μL of 20% Tween-80 were added to each well, and the plates were further incubated overnight.[40] Fluorescence was measured by excitation at 530 nm and emission at 590 nm, using a POLARstar Omega plate reader (BMG Labtech). To determine the compound MIC values, 2 μL of 2-fold serial dilutions of 50× DMSO solutions of the compounds was transferred to the assay plates, leaving a row of wells around the edge of the plate filled with water as a humidity barrier. The remainder of the assay was performed as above for single-concentration screening. The pMV261 expression system is also compatible with *M. tuberculosis* and permitted measurement of compound MIC values in *M. tuberculosis* as described[40] with slight modifications: the inoculum was 1×10^5 CFU/mL, and the growth medium was Middlebrook 7H9 supplemented with 10% (v/v) OADC and 0.025% (v/v) Tween-80.

Generation of *M. bovis* BCG Spontaneous Mutants. *M. bovis* BCG was grown on Middlebrook 7H11 agar plates (Difco) supplemented with 10% (v/v) OADC (Sigma) and 0.5% (v/v) glycerol or in liquid medium in Middlebrook 7H9 broth (Difco), containing 0.05% (v/v) Tween-80, 10% (v/v) OADC, and 0.25% (v/v) glycerol. The MIC values of the compounds on solid medium were first determined by plating out 10 μL of dilutions of 10^4, 10^3, 10^2, and 10^1 of mid log phase bacteria onto the agar plates with increasing concentrations of compound. *M. bovis* BCG spontaneous mutants were generated by plating 10^8 mid log cells ($A_{600\,nm}$ of 0.8–1.0) onto agar plates containing 2.5 , 5, and 10 times the MIC of each compound. A strain with a *recG* mutation, which could theoretically increase mutation frequency, was also tested. Colonies appeared after 2−4 weeks of incubation at 37 °C in a CO_2 incubator and were picked and grown to mid log phase in liquid medium at 37 °C. Resistance was confirmed by plating 10 μL of bacteria onto agar plates containing 5 times the MIC of the compound. Resistant mutants and the parental strains were grown to mid log phase in 10 mL of liquid medium at 2 times the MIC of the compound for the mutant strains but no compound for the parent strains. Following genomic DNA extraction from each resistant mutant and the parental strains, Mt-*dprE1* was amplified by PCR using the primers 5′-CCGAATTGTGCAGGTAGC-3′ and 5′-GGCACCGCCACG-GTAATC-3′ and sequenced using the same primers by Eurofins MWG Operon, Ebersberg, Germany. Point mutations were identified using the EMBL-EBI pairwise sequence alignment tool (http://www.ebi.ac.uk/Tools/psa/emboss_needle/nucleotide.html).

Time-Lapse Microscopy. A recombinant *M. tuberculosis* strain carrying the integrative plasmid pND235 expressing GFP[29] was grown to mid log phase. Bacteria were collected and concentrated 10-fold by centrifugation, and single-cell suspensions were prepared by passing the cells through a 5 μm filter to

remove clumps. Bacteria were grown and imaged in a microfluidic device as described previously.[29] Images were acquired every 60 min on the phase and fluorescent channels using a PersonalDV imaging system (Applied Precision, GE Healthcare) equipped with a 100× objective (1.30 NA, 0.2 mm WD) and a CoolSnap HQ2 CCD camera. Bacteria were initially grown in complete Middlebrook 7H9 medium until they formed small microcolonies, after which they were exposed to GSK059 for 7 days. Fresh medium (with or without compound) was supplemented every 24 h. Analysis and annotation of the image sequences was carried out using ImageJ v 1.47a (http://rsb.info.nih.gov/ij/).

Data Analysis. Enzyme kinetic data and FAD fluorescence quenching data were fitted using the nonlinear curve-fitting program GraFit version 7.0.3 (Erithacus Software Ltd., Surrey, UK). Dose−response curve data were fitted to eq 1

$$v_i = \frac{(a - d)}{1 + \left(\frac{[I]}{IC_{50}}\right)^h} + d \tag{1}$$

where v_i is the rate, a is the uninhibited value, d is the fully inhibited value, $[I]$ is the inhibitor concentration, IC_{50} is the $[I]$ that gives $1/2 \times (a - d)$, and h is the Hill coefficient. For compounds showing an IC_{50} of less than the enzyme concentration, the same dose−response curve data were also fitted to eq 2

$$\frac{v_i}{v_0} = 1 - \frac{([E] + [I] + K_i^{app}) - \sqrt{([E] + [I] + K_i^{app})^2 - 4[E][I]}}{2[E]} + c \tag{2}$$

where v_0 and v_i are the rates in the absence and presence of inhibitor, respectively, $[E]$ is the total active enzyme concentration, K_i^{app} is the apparent inhibition constant, $[I]$ is the concentration of inhibitor, and c is the fully inhibited background rate.[38]

FAD fluorescence quenching curves were fitted to eq 3

$$F_{obs} = F_0\left[1 - \frac{([E] + [I] + K_d^{app}) - \sqrt{([E] + [I] + K_d^{app})^2 - 4[E][I]}}{2[E]}\right] + c \tag{3}$$

where F_{obs} and F_0 are the normalized fluorescence intensities in the absence and presence of inhibitor, respectively, $[E]$ is the total active enzyme concentration, K_d^{app} is the apparent dissociation constant, $[I]$ is the concentration of inhibitor, and c is F_{obs} at infinite $[I]$. E was fixed at 2.9 μM except for tight-binding compounds (GSK710, GSK058, GSK059, and GSK310), where E was floated. Screening data were analyzed using the ActivityBase Suite (ID Business Solutions Ltd., Surrey, UK). Single-concentration screening data were expressed as percent inhibition.

ASSOCIATED CONTENT

S **Supporting Information**

The Supporting Information is available free of charge on the ACS Publications website at DOI: 10.1021/acsinfecdis.5b00065

> Figure S1 shows resistance data by spontaneous mutations; Table S1 shows inhibitors of Mt-DprE1 identified by screening the TB-set using the enzymatic assay; additional experimental procedures (PDF)

W **Web-Enhanced Features**

Movie S1 shows the effect of treatment of *M. tuberculosis* with 40 μM GSK059 monitored by time-lapse microscopy.

AUTHOR INFORMATION

Corresponding Authors

*(L.B.) E-mail: lluis.p.ballell@gsk.com (for compound queries).
*(G.S.B.) E-mail: G.Besra@bham.ac.uk (for biological constructs).
*(A.A.) E-mail: argyrides.x.argyrou@gsk.com (any other queries).

Author Contributions

A.A. carried out the enzyme assays and oversaw all aspects of the project and manuscript preparation. S.M.B. carried out the multicopy suppressor screen and isolated the spontaneous resistant mutants. M.C.I., J.C.P., and R.J.Y. carried out and coordinated the chemical synthesis of compounds. C.J.S. and J.P.H. carried out the binding assays. L.V.-G.D.P. carried out the enzyme assay screen. E.P.H. carried out the MIC measurements in *M. tuberculosis*. N.D. carried out the time-lapse microscopy experiments. B.M. performed protein expression. M.R. purified the enzyme. L.B., G.S.B., and A.A. wrote the manuscript with input from all authors.

Notes

The authors declare no competing financial interest.

ABBREVIATIONS

TB, tuberculosis; MDR-TB, multidrug-resistant tuberculosis; XDR-TB, extremely drug-resistant tuberculosis; Mt-DprE1, *Mycobacterium tuberculosis* decaprenylphosphoryl-β-D-ribose oxidase; DPR, decaprenylphosphoryl-β-D-ribose; DPX, decaprenylphosphoryl-β-D-2′-keto-*erythro*-pentafuranose; DPA, decaprenylphosphoryl-β-D-arabinose; FPR, farnesylphosphoryl-β-D-ribose; FPX, farnesylphosphoryl-β-D-2′-keto-*erythro*-pentafuranose; MIC, minimum inhibitory concentration; FAD, flavin adenine dinucleotide; Hepes, *N*-(2-hydroxyethyl)piperazine-*N*′-(2-ethanesulfonic acid); DMSO, dimethyl sulfoxide; HPLC, high-performance liquid chromatrography; LC-MS, liquid chromatography−mass spectrometry; NMR, nuclear magnetic resonance

REFERENCES

(1) Gler, M. T., Skripconoka, V., Sanchez-Garavito, E., Xiao, H., Cabrera-Rivero, J. L., Vargas-Vasquez, D. E., Gao, M., Awad, M., Park, S. K., Shim, T. S., Suh, G. Y., Danilovits, M., Ogata, H., Kurve, A., Chang, J., Suzuki, K., Tupasi, T., Koh, W. J., Seaworth, B., Geiter, L. J., and Wells, C. D. (2012) Delamanid for multidrug-resistant pulmonary tuberculosis. *N. Engl. J. Med. 366*, 2151−2160.

(2) Zumla, A., Nahid, P., and Cole, S. T. (2013) Advances in the development of new tuberculosis drugs and treatment regimens. *Nat. Rev. Drug Discovery 12*, 388−404.

(3) Wright, A., Zignol, M., Van Deun, A., Falzon, D., Gerdes, S. R., Feldman, K., Hoffner, S., Drobniewski, F., Barrera, L., van Soolingen, D., Boulabhal, F., Paramasivan, C. N., Kam, K. M., Mitarai, S., Nunn, P., and Raviglione, M. (2009) Epidemiology of antituberculosis drug resistance 2002−07: an updated analysis of the global project on anti-tuberculosis drug resistance surveillance. *Lancet 373*, 1861−1873.

(4) Ballell, L., Bates, R. H., Young, R. J., Alvarez-Gomez, D., Alvarez-Ruiz, E., Barroso, V., Blanco, D., Crespo, B., Escribano, J., Gonzalez, R., Lozano, S., Huss, S., Santos-Villarejo, A., Martin-Plaza, J. J., Mendoza, A., Rebollo-Lopez, M. J., Remuinan-Blanco, M., Lavandera, J. L., Perez-Herran, E., Gamo-Benito, F. J., Garcia-Bustos, J. F., Barros, D., Castro, J. P., and Cammack, N. (2013) Fueling open-source drug discovery: 177 small-molecule leads against tuberculosis. *ChemMedChem 8*, 313−321.

(5) Remuinan, M. J., Perez-Herran, E., Rullas, J., Alemparte, C., Martinez-Hoyos, M., Dow, D. J., Afari, J., Mehta, N., Esquivias, J., Jimenez, E., Ortega-Muro, F., Fraile-Gabaldon, M. T., Spivey, V. L., Loman, N. J., Pallen, M. J., Constantinidou, C., Minick, D. J., Cacho, M., Rebollo-Lopez, M. J., Gonzalez, C., Sousa, V., Angulo-Barturen, I., Mendoza-Losana, A., Barros, D., Besra, G. S., Ballell, L., and Cammack, N. (2013) Tetrahydropyrazolo[1,5-*a*]pyrimidine-3-carboxamide and *N*-benzyl-6′,7′-dihydrospiro[piperidine-4,4′-thieno[3,2-*c*]pyran] analogues with bactericidal efficacy against *Mycobacterium tuberculosis* targeting MmpL3. *PLoS One 8*, e60933.

(6) Abrahams, K. A., Cox, J. A., Spivey, V. L., Loman, N. J., Pallen, M. J., Constantinidou, C., Fernandez, R., Alemparte, C., Remuinan, M. J., Barros, D., Ballell, L., and Besra, G. S. (2012) Identification of novel imidazo[1,2-*a*]pyridine inhibitors targeting *M. tuberculosis* QcrB. *PLoS One 7*, e52951.

(7) Encinas, L., O'Keefe, H., Neu, M., Remuinan, M. J., Patel, A. M., Guardia, A., Davie, C. P., Perez-Macias, N., Yang, H., Convery, M. A., Messer, J. A., Perez-Herran, E., Centrella, P. A., Alvarez-Gomez, D., Clark, M. A., Huss, S., O'Donovan, G. K., Ortega-Muro, F., McDowell, W., Castaneda, P., Arico-Muendel, C. C., Pajk, S., Rullas, J., Angulo-Barturen, I., Alvarez-Ruiz, E., Mendoza-Losana, A., Ballell Pages, L., Castro-Pichel, J., and Evindar, G. (2014) Encoded library technology as a source of hits for the discovery and lead optimization of a potent and selective class of bactericidal direct inhibitors of *Mycobacterium tuberculosis* InhA. *J. Med. Chem. 57*, 1276−1288.

(8) Knapp, S., Arruda, P., Blagg, J., Burley, S., Drewry, D. H., Edwards, A., Fabbro, D., Gillespie, P., Gray, N. S., Kuster, B., Lackey, K. E., Mazzafera, P., Tomkinson, N. C., Willson, T. M., Workman, P., and Zuercher, W. J. (2013) A public-private partnership to unlock the untargeted kinome. *Nat. Chem. Biol. 9*, 3−6.

(9) Mikusova, K., Huang, H., Yagi, T., Holsters, M., Vereecke, D., D'Haeze, W., Scherman, M. S., Brennan, P. J., McNeil, M. R., and Crick, D. C. (2005) Decaprenylphosphoryl arabinofuranose, the donor of the D-arabinofuranosyl residues of mycobacterial arabinan, is formed via a two-step epimerization of decaprenylphosphoryl ribose. *J. Bacteriol. 187*, 8020−8025.

(10) Wolucka, B. A., McNeil, M. R., de Hoffmann, E., Chojnacki, T., and Brennan, P. J. (1994) Recognition of the lipid intermediate for arabinogalactan/arabinomannan biosynthesis and its relation to the mode of action of ethambutol on mycobacteria. *J. Biol. Chem. 269*, 23328−23335.

(11) Alderwick, L. J., Radmacher, E., Seidel, M., Gande, R., Hitchen, P. G., Morris, H. R., Dell, A., Sahm, H., Eggeling, L., and Besra, G. S. (2005) Deletion of Cg-emb in corynebacterianeae leads to a novel truncated cell wall arabinogalactan, whereas inactivation of Cg-ubiA results in an arabinan-deficient mutant with a cell wall galactan core. *J. Biol. Chem. 280*, 32362−32371.

(12) Kolly, G. S., Boldrin, F., Sala, C., Dhar, N., Hartkoorn, R. C., Ventura, M., Serafini, A., McKinney, J. D., Manganelli, R., and Cole, S. T. (2014) Assessing the essentiality of the decaprenyl-phospho-D-arabinofuranose pathway in *Mycobacterium tuberculosis* using conditional mutants. *Mol. Microbiol. 92*, 194−211.

(13) Brecik, M., Centarova, I., Mukherjee, R., Kolly, G. S., Huszar, S., Bobovska, A., Kilacskova, E., Mokosova, V., Svetlikova, Z., Sarkan, M., Neres, J., Kordulakova, J., Cole, S. T., and Mikusova, K. (2015) DprE1 is a vulnerable tuberculosis drug target due to its cell wall localization. *ACS Chem. Biol. 10*, 1631−1636.

(14) Makarov, V., Manina, G., Mikusova, K., Mollmann, U., Ryabova, O., Saint-Joanis, B., Dhar, N., Pasca, M. R., Buroni, S., Lucarelli, A. P., Milano, A., De, R. E., Belanova, M., Bobovska, A., Dianiskova, P., Kordulakova, J., Sala, C., Fullam, E., Schneider, P., McKinney, J. D., Brodin, P., Christophe, T., Waddell, S., Butcher, P., Albrethsen, J.,

Rosenkrands, I., Brosch, R., Nandi, V., Bharath, S., Gaonkar, S., Shandil, R. K., Balasubramanian, V., Balganesh, T., Tyagi, S., Grosset, J., Riccardi, G., and Cole, S. T. (2009) Benzothiazinones kill *Mycobacterium tuberculosis* by blocking arabinan synthesis. *Science 324*, 801−804.

(15) Batt, S. M., Jabeen, T., Bhowruth, V., Quill, L., Lund, P. A., Eggeling, L., Alderwick, L. J., Futterer, K., and Besra, G. S. (2012) Structural basis of inhibition of *Mycobacterium tuberculosis* DprE1 by benzothiazinone inhibitors. *Proc. Natl. Acad. Sci. U. S. A. 109*, 11354−11359.

(16) Chatterji, M., Shandil, R., Manjunatha, M. R., Solapure, S., Ramachandran, V., Kumar, N., Saralaya, R., Panduga, V., Reddy, J., Kr, P., Sharma, S., Sadler, C., Cooper, C. B., Mdluli, K., Iyer, P. S., Narayanan, S., and Shirude, P. S. (2014) 1,4-Azaindole, a potential drug candidate for treatment of tuberculosis. *Antimicrob. Agents Chemother. 58*, 5325−5331.

(17) Naik, M., Humnabadkar, V., Tantry, S. J., Panda, M., Narayan, A., Guptha, S., Panduga, V., Manjrekar, P., Jena, L. K., Koushik, K., Shanbhag, G., Jatheendranath, S., Manjunatha, M. R., Gorai, G., Bathula, C., Rudrapatna, S., Achar, V., Sharma, S., Ambady, A., Hegde, N., Mahadevaswamy, J., Kaur, P., Sambandamurthy, V. K., Awasthy, D., Narayan, C., Ravishankar, S., Madhavapeddi, P., Reddy, J., Prabhakar, K., Saralaya, R., Chatterji, M., Whiteaker, J., McLaughlin, B., Chiarelli, L. R., Riccardi, G., Pasca, M. R., Binda, C., Neres, J., Dhar, N., Signorino-Gelo, F., McKinney, J. D., Ramachandran, V., Shandil, R., Tommasi, R., Iyer, P. S., Narayanan, S., Hosagrahara, V., Kavanagh, S., Dinesh, N., and Ghorpade, S. R. (2014) 4-Aminoquinolone piperidine amides: noncovalent inhibitors of DprE1 with long residence time and potent antimycobacterial activity. *J. Med. Chem. 57*, 5419−5434.

(18) Panda, M., Ramachandran, S., Ramachandran, V., Shirude, P. S., Humnabadkar, V., Nagalapur, K., Sharma, S., Kaur, P., Guptha, S., Narayan, A., Mahadevaswamy, J., Ambady, A., Hegde, N., Rudrapatna, S. S., Hosagrahara, V. P., Sambandamurthy, V. K., and Raichurkar, A. (2014) Discovery of pyrazolopyridones as a novel class of noncovalent DprE1 inhibitor with potent anti-mycobacterial activity. *J. Med. Chem. 57*, 4761−4771.

(19) Shirude, P. S., Shandil, R. K., Manjunatha, M. R., Sadler, C., Panda, M., Panduga, V., Reddy, J., Saralaya, R., Nanduri, R., Ambady, A., Ravishankar, S., Sambandamurthy, V. K., Humnabadkar, V., Jena, L. K., Suresh, R. S., Srivastava, A., Prabhakar, K. R., Whiteaker, J., McLaughlin, R. E., Sharma, S., Cooper, C. B., Mdluli, K., Butler, S., Iyer, P. S., Narayanan, S., and Chatterji, M. (2014) Lead optimization of 1,4-azaindoles as antimycobacterial agents. *J. Med. Chem. 57*, 5728−5737.

(20) Shirude, P. S., Shandil, R., Sadler, C., Naik, M., Hosagrahara, V., Hameed, S., Shinde, V., Bathula, C., Humnabadkar, V., Kumar, N., Reddy, J., Panduga, V., Sharma, S., Ambady, A., Hegde, N., Whiteaker, J., McLaughlin, R. E., Gardner, H., Madhavapeddi, P., Ramachandran, V., Kaur, P., Narayan, A., Guptha, S., Awasthy, D., Narayan, C., Mahadevaswamy, J., Vishwas, K. G., Ahuja, V., Srivastava, A., Prabhakar, K. R., Bharath, S., Kale, R., Ramaiah, M., Choudhury, N. R., Sambandamurthy, V. K., Solapure, S., Iyer, P. S., Narayanan, S., and Chatterji, M. (2013) Azaindoles: noncovalent DprE1 inhibitors from scaffold morphing efforts, kill *Mycobacterium tuberculosis* and are efficacious *in vivo. J. Med. Chem. 56*, 9701−9708.

(21) Wang, F., Sambandan, D., Halder, R., Wang, J., Batt, S. M., Weinrick, B., Ahmad, I., Yang, P., Zhang, Y., Kim, J., Hassani, M., Huszar, S., Trefzer, C., Ma, Z., Kaneko, T., Mdluli, K. E., Franzblau, S., Chatterjee, A. K., Johnsson, K., Mikusova, K., Besra, G. S., Futterer, K., Robbins, S. H., Barnes, S. W., Walker, J. R., Jacobs, W. R., Jr., and Schultz, P. G. (2013) Identification of a small molecule with activity against drug-resistant and persistent tuberculosis. *Proc. Natl. Acad. Sci. U. S. A. 110*, E2510−E2517.

(22) Neres, J., Hartkoorn, R. C., Chiarelli, L. R., Gadupudi, R., Pasca, M. R., Mori, G., Venturelli, A., Savina, S., Makarov, V., Kolly, G. S., Molteni, E., Binda, C., Dhar, N., Ferrari, S., Brodin, P., Delorme, V., Landry, V., de Jesus Lopes Ribeiro, A. L., Farina, D., Saxena, P., Pojer, F., Carta, A., Luciani, R., Porta, A., Zanoni, G., De, R. E., Costi, M. P., Riccardi, G., and Cole, S. T. (2015) 2-Carboxyquinoxalines kill *Mycobacterium tuberculosis* through noncovalent inhibition of DprE1. *ACS Chem. Biol. 10*, 705−714.

(23) Goldman, R. C. (2013) Why are membrane targets discovered by phenotypic screens and genome sequencing in *Mycobacterium tuberculosis*? *Tuberculosis 93*, 569−588.

(24) Li, X., Zolli-Juran, M., Cechetto, J. D., Daigle, D. M., Wright, G. D., and Brown, E. D. (2004) Multicopy suppressors for novel antibacterial compounds reveal targets and drug efflux susceptibility. *Chem. Biol. 11*, 1423−1430.

(25) Luesch, H., Wu, T. Y., Ren, P., Gray, N. S., Schultz, P. G., and Supek, F. (2005) A genome-wide overexpression screen in yeast for small-molecule target identification. *Chem. Biol. 12*, 55−63.

(26) Stover, C. K., de la Cruz, V. F., Fuerst, T. R., Burlein, J. E., Benson, L. A., Bennett, L. T., Bansal, G. P., Young, J. F., Lee, M. H., and Hatfull, G. F. (1991) New use of BCG for recombinant vaccines. *Nature 351*, 456−460.

(27) Franzblau, S. G., Witzig, R. S., McLaughlin, J. C., Torres, P., Madico, G., Hernandez, A., Degnan, M. T., Cook, M. B., Quenzer, V. K., Ferguson, R. M., and Gilman, R. H. (1998) Rapid, low-technology MIC determination with clinical *Mycobacterium tuberculosis* isolates by using the microplate alamar blue assay. *J. Clin. Microbiol. 36*, 362−366.

(28) Neres, J., Pojer, F., Molteni, E., Chiarelli, L. R., Dhar, N., Boy-Rottger, S., Buroni, S., Fullam, E., Degiacomi, G., Lucarelli, A. P., Read, R. J., Zanoni, G., Edmondson, D. E., De, R. E., Pasca, M. R., McKinney, J. D., Dyson, P. J., Riccardi, G., Mattevi, A., Cole, S. T., and Binda, C. (2012) Structural basis for benzothiazinone-mediated killing of *Mycobacterium tuberculosis*. *Sci. Transl. Med. 4*, 150ra121.

(29) Wakamoto, Y., Dhar, N., Chait, R., Schneider, K., Signorino-Gelo, F., Leibler, S., and McKinney, J. D. (2013) Dynamic persistence of antibiotic-stressed mycobacteria. *Science 339*, 91−95.

(30) Guo, H., Seet, Q., Denkin, S., Parsons, L., and Zhang, Y. (2006) Molecular characterization of isoniazid-resistant clinical isolates of *Mycobacterium tuberculosis* from the USA. *J. Med. Microbiol. 55*, 1527−1531.

(31) Hiramatsu, K. (2001) Vancomycin-resistant *Staphylococcus aureus*: a new model of antibiotic resistance. *Lancet Infect. Dis. 1*, 147−155.

(32) Flensburg, J., and Skold, O. (1987) Massive overproduction of dihydrofolate reductase in bacteria as a response to the use of trimethoprim. *Eur. J. Biochem. 162*, 473−476.

(33) Banerjee, A., Dubnau, E., Quemard, A., Balasubramanian, V., Um, K. S., Wilson, T., Collins, D., de, L. G., and Jacobs, W. R., Jr. (1994) *InhA*, a gene encoding a target for isoniazid and ethionamide in *Mycobacterium tuberculosis*. *Science 263*, 227−230.

(34) Shi, W., Zhang, X., Jiang, X., Yuan, H., Lee, J. S., Barry, C. E., III, Wang, H., Zhang, W., and Zhang, Y. (2011) Pyrazinamide inhibits trans-translation in *Mycobacterium tuberculosis*. *Science 333*, 1630−1632.

(35) Bunnage, M. E., Chekler, E. L., and Jones, L. H. (2013) Target validation using chemical probes. *Nat. Chem. Biol. 9*, 195−199.

(36) Simon, G. M., Niphakis, M. J., and Cravatt, B. F. (2013) Determining target engagement in living systems. *Nat. Chem. Biol. 9*, 200−205.

(37) Depardieu, F., Podglajen, I., Leclercq, R., Collatz, E., and Courvalin, P. (2007) Modes and modulations of antibiotic resistance gene expression. *Clin. Microbiol. Rev. 20*, 79−114.

(38) Copeland, R. A. (2005) Tight binding inhibition. In *Evaluation of Enzyme Inhibitors in Drug Discovery: A Guide for Medicinal Chemists and Pharmacologists*, pp 178−213, Wiley, Hoboken, NJ, USA.

(39) Harbury, H. A., Lanoue, K. F., Loach, P. A., and Amick, R. M. (1959) Molecular interaction of isoalloxazine derivatives. II. *Proc. Natl. Acad. Sci. U. S. A. 45*, 1708−1717.

(40) Taneja, N. K., and Tyagi, J. S. (2007) Resazurin reduction assays for screening of anti-tubercular compounds against dormant and actively growing *Mycobacterium tuberculosis*, *Mycobacterium bovis* BCG and *Mycobacterium smegmatis*. *J. Antimicrob. Chemother. 60*, 288−293.